Long-wave Marangoni instability in a binary liquid layer on a thick solid substrate

A. Podolny,[1] A. A. Nepomnyashchy,[1,2] and A. Oron[3]
[1]*Department of Mathematics, Technion–Israel Institute of Technology, Haifa 32000, Israel*
[2]*Minerva Center for Nonlinear Physics of Complex System, Technion–Israel Institute of Technology, Haifa 32000, Israel*
[3]*Department of Mechanical Engineering, Technion–Israel Institute of Technology, Haifa 32000, Israel*
(Received 5 December 2006; revised manuscript received 17 May 2007; published 20 August 2007)

We consider a system which consists of a layer of an incompressible binary liquid with a deformable free surface, and a thick solid substrate subjected to a differential heating across it. We investigate the long-wave thermosolutal Marangoni instability in the case of asymptotically small Lewis and Galileo numbers for finite capillary and Biot numbers with the Soret effect taken into account. We find both long-wave monotonic and oscillatory modes of instability in various parameter domains of Biot and Soret numbers. In the domain of finite wave numbers the monotonic instability is found, but the minimum of the monotonic neutral curve is shown to be located in the long-wave region. A set of nonlinear evolution equations is derived for the description of the spatiotemporal dynamics of the oscillatory instability. The weakly nonlinear analysis is carried out for the monotonic instability.

DOI: 10.1103/PhysRevE.76.026309 PACS number(s): 47.20.Dr, 47.55.dm, 47.55.pf

I. INTRODUCTION

Various transport processes encountered in technology and nature are due to or affected by simultaneous action of temperature and solute concentration gradients. Different configurations of these gradients were discussed [1] in the context of buoyancy-driven convection. Similar settings can be also considered in regards with the surface-tension-driven or Marangoni convection in the no-gravity environment. Relevant examples are different techniques of materials processing, e.g., crystal growth, from binary or multicomponent liquid mixtures. Many of them, especially those employing the floating zone and temperature-gradient methods, involve large temperature and possibly concentration gradients imposed in various directions relatively to the melt [1].

The concentration gradient across the layer can be either imposed independently of the temperature gradient or generated by the Soret effect. The case where the solute concentration is produced by the Soret effect and deformations were neglected, was considered in Refs. [2–9]. Unlike in the case of a pure liquid, an oscillatory Marangoni instability is possible in binary liquids due to the presence of two instability mechanisms related to both temperature and solute concentration gradients [2,4,5].

Surface deformation can lead to the emergence of a *new* long-wave stationary instability mode. In both cases of independent temperature and concentration gradients [11] and that of the concentration gradient induced by the Soret effect [12], it was found that for sufficiently small values of the Galileo number (under reduced gravity for thin layers), the neutral stability curve has an additional minimum at zero value of the wave number $k=0$, with the critical Marangoni number proportional to the Galileo number.

Bhattacharjee [12] considered the Marangoni instability in binary-liquid mixtures when the temperature of the substrate is specified. He found that in the long-wave limit and for a small Biot number at the free surface the monotonic instability emerges. Also, the oscillatory instability in the limit of a small Lewis number was found emerging only in the finite-wavelength domain when the separation ratio (the Soret number) is confined to a certain domain. We note that in spite of the fact that Bhattacharjee [12] derived general expressions for both monotonic and oscillatory instability thresholds in the case of a finite Biot number, the analysis of this general case was not carried out.

Joo [13] investigated the stability of a binary-liquid layer heated at the deformable gas-liquid interface side in the presence of the Soret effect when the temperature of the substrate is fixed. In this case the instability is driven by solutocapillarity and retarded by thermocapillarity. As in Ref. [12], the general characteristic relation between the thermal and solutal Marangoni numbers was obtained assuming that all parameters of the problem, such as the wave number of the perturbation and the Biot and capillary numbers, are of the unity order. However, the detailed analysis was presented only in the limit of a small Biot number.

Podolny *et al.* [14] developed the theory of the long-wave Marangoni instability in a binary-liquid layer with a deformable interface in the limit of a small Biot number B and specified heat flux at the liquid-solid interface in the presence of the Soret effect. The condition of a specified heat flux at the solid-liquid interface corresponds to the limit of a low thermal conductivity of the solid substrate. It was shown [14] that the problem was characterized by two distinct asymptotic limits for the disturbance wave number k, which are $k \sim B^{1/4}$ and $k \sim B^{1/2}$, caused by the presence of two instability mechanisms, namely, thermocapillary and solutocapillary effects. The asymptotic limit of $k \sim B^{1/2}$ found there was novel and was unknown for pure liquids. A diversity of instability modes was revealed [14]. Specifically, a new long-wave oscillatory mode was found for sufficiently small values of the Galileo number.

Furthermore, the investigation was extended to the case of a finite Biot number at the upper free deformable surface [15] and zero Biot number at the bottom rigid plane. As the mass flux at the boundaries of the layer vanishes, the effective Sherwood number which represents a mass-transfer analog of the Biot number is zero. Therefore, this was a basis for a conjecture that in spite of a finite value of the Biot number, the long-wave instability would emerge. Our conjecture was found correct and various types of both long-wave monotonic and oscillatory modes of instability in various param-

eter domains were discovered. Also, a set of nonlinear long-wave equations for the oscillatory instability was derived in the limit of both small Lewis and Galileo numbers. An oscillatory instability was found for small wave numbers $k=O(\sqrt{L})\ll 1$. In the case of small gravity, three-dimensional stable supercritical wavy patterns were found.

In the present paper, we consider the most general case of a system that consists of a layer of an incompressible binary liquid with a deformable free surface, and a thick solid substrate of an arbitrary thermal conductivity heated or cooled from below. As we will show, the problem is now determined by two independent Biot numbers, the Biot number B characterizing the heat transfer on the free surface, and effective Biot number b on the liquid-solid interface. Both Biot numbers are generally finite. We will see that the influence of the finite bottom Biot number on the linear stability is crucial. Also, in contradistinction with the previous papers on this subject, we target the nonlinear dynamics of both oscillatory and monotonic instability modes.

The structure of the paper is as follows. In Sec. II we solve the heat transfer problem in the solid substrate and formulate the closed problem for the liquid layer in terms of the effective Biot number at the bottom, which depends on the wave number and growth rate of the disturbance. In Sec. III we investigate the long-wave Marangoni instability in the case of asymptotically small Lewis and Galileo numbers for all finite capillary and Biot numbers at the gas-liquid and liquid-solid interfaces. In the framework of long-wave linear stability theory, we find both monotonic and oscillatory modes of instability in various parameter domains of Biot and Soret numbers.

The linear theory for monotonic instability has been also developed for finite wave numbers. Our analysis shows that in the case of small Galileo and Lewis numbers, there are no additional minima of the neutral curve in the region $k=O(1)$. We show that the minimum of the monotonic neutral curve is located either at $k=0$ or in the long-wave domain $k=O(L^{1/4})$. The results of intermediate asymptotics for the monotonic instability threshold in the domain $k=O(L^{1/4})$ perfectly match both the long-wave limit, $k=O(\sqrt{L})$, and the limit of finite wave numbers $k=O(1)$. Section IV is devoted to the nonlinear analysis of the problem for long waves with $k=O(L^{1/2})$. Nonlinear evolution equations describing the dynamics of the long-wave monotonic instability in the domain $\sqrt{L}\ll k\ll 1$ are derived in Sec. V. It is shown that the analysis of the monotonic instability in the region above the threshold requires a new scaling of the wave number which is different from that in the case of the oscillatory instability. A weakly nonlinear analysis for the case of the monotonic instability leads in Sec. V to the derivation of the evolution equation similar to that derived in Ref. [18] for the Bénard-Marangoni instability in pure liquids.

II. STATEMENT OF THE PROBLEM AND GOVERNING EQUATIONS

A. Mathematical model

We consider a layer of an incompressible binary liquid of horizontally infinite extent at rest on a solid substrate of a finite thickness h_s heated or cooled from below in the gravity field. The liquid layer is exposed to the ambient gas phase at its deformable free surface (Fig. 1). Surface tension σ is assumed to depend upon both temperature ϑ and solute concentration c, $\sigma=\sigma(\vartheta,c)$, and, therefore, Marangoni (both thermocapillary and solutocapillary) effects are taken into account. It is assumed that the layer is sufficiently thin, so that the effect of buoyancy can be neglected as compared to the Marangoni effect.

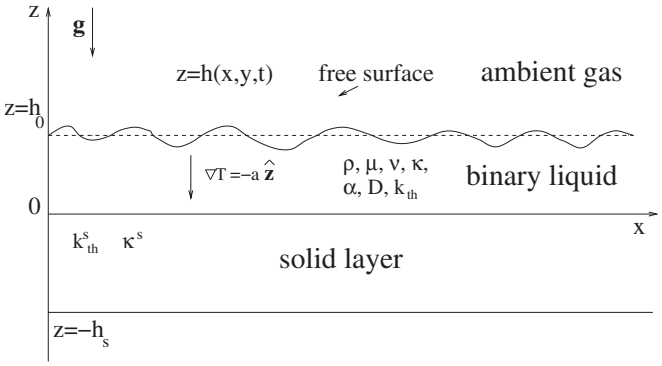

FIG. 1. Sketch of the system.

As a generalization of the standard model of heat and mass transfer given by the Fourier's and Fick's laws, where the heat and mass fluxes are taken proportional to the temperature and concentration gradients, respectively, one may consider both fluxes to be each linear combinations of both of these gradients [10]. This extended model incorporates the Soret and Dufour effects. However, the Dufour effect is exceedingly weak in liquids and can be safely neglected, while the Soret effect can be significant and will be taken into account hereafter. Therefore, in what follows, the heat $\vec{J}_h$ and mass $\vec{J}_m$ fluxes are given by

$$\vec{J}_h=-\lambda\vec{\nabla}\vartheta,\quad \vec{J}_m=-\rho D(\vec{\nabla}c+\alpha\vec{\nabla}\vartheta), \tag{1}$$

respectively, where ϑ and c are the fluid temperature and solute concentration, respectively, ρ, λ, D, α represent density, thermal conductivity, mass diffusivity, and the Soret coefficient of the binary mixture, respectively. Note that one more parameter, namely, the Soret diffusion parameter S_T, associated with the Soret effect is also known in the literature [19]. It is related to the Soret coefficient α via the relationship $\alpha=S_T/c_{\mathrm{wt}}$, where c_{wt} is a weight concentration of the mixture.

A set of governing equations consists of the two-dimensional set of hydrodynamic equations for an incompressible liquid, as well as heat and mass transfer equations in the presence of the Soret effect,

$$\vec{\nabla}\cdot\mathbf{v}=0, \tag{2a}$$

$$\mathbf{v}_t+(\mathbf{v}\cdot\vec{\nabla})\mathbf{v}=-\rho^{-1}\vec{\nabla}p+\nu\vec{\nabla}^2\mathbf{v}-g\mathbf{e}_z, \tag{2b}$$

$$\vartheta_t+\mathbf{v}\cdot\vec{\nabla}\vartheta=\kappa\vec{\nabla}^2\vartheta, \tag{2c}$$

$$c_t + \mathbf{v}\cdot\vec{\nabla}c = D\vec{\nabla}^2 c + \alpha D\vec{\nabla}^2\vartheta. \tag{2d}$$

Here $\mathbf{v}$, p are fields of the fluid velocity, and pressure, respectively, ν, κ are, respectively, kinematic viscosity, and thermal diffusivity of the binary mixture, $\vec{\nabla}\equiv(\partial_x,\partial_z)$, and t is time.

In the solid substrate, the heat equation is

$$\vartheta_t^s = \kappa^s\vec{\nabla}^2\vartheta^s, \tag{3}$$

where ϑ^s and κ^s are the temperature and thermal diffusivity in the solid, respectively.

The boundary conditions at the liquid-solid interface $z=0$ include the no-slip, no-penetration condition for the fluid velocity, continuity of the normal components of the heat flux and the temperature at the solid-liquid interface, and mass impermeability, respectively,

$$z=0:\mathbf{v}=0,\quad \lambda\vartheta_z=\lambda^s\vartheta_z^s,\quad \vartheta=\vartheta^s,\quad c_z=-\alpha\vartheta_z, \tag{4}$$

where λ^s is thermal conductivity of the solid.

The boundary condition at the solid-gas interface $z=-h_s$ reflects the fact that a constant temperature is imposed at the bottom of the solid substrate

$$\vartheta^s=\vartheta_-. \tag{5}$$

At the free liquid-gas interface $z=h(x,y,t)$, the boundary conditions are, respectively, the kinematic boundary condition, that of heat transfer governed by the Newton's law of cooling and mass impermeability, respectively,

$$\frac{\partial h}{\partial t}+\frac{\partial h}{\partial x}u+\frac{\partial h}{\partial y}v=w, \tag{6a}$$

$$\lambda\vec{\nabla}\vartheta\cdot\mathbf{n}+q(\vartheta-\vartheta_+)=0, \tag{6b}$$

$$\lambda\vec{\nabla}c\cdot\mathbf{n}-\alpha\cdot q(\vartheta-\vartheta_+)=0, \tag{6c}$$

where $\mathbf{v}=(u,v,w)$, q is the heat transfer coefficient describing the rate of heat transfer from the liquid to the ambient gas phase at the constant temperature ϑ_+, and $\mathbf{n}$ is the unit outward vector normal to the interface.

Furthermore, at the liquid-gas free surface $z=h(x,y,t)$, the balance of both normal and tangential interfacial stresses is given, respectively, as

$$-p+\frac{2\mu}{1+h_x^2+h_y^2}[u_x(h_x^2-1)+v_y(h_y^2-1)-h_x(u_z+w_x)+(u_y+v_x)h_xh_y-(w_y+v_z)h_y]=\sigma\frac{h_{xx}(1+h_y^2)+h_{yy}(1+h_x^2)-2h_xh_yh_{xy}}{(1+h_x^2+h_y^2)^{3/2}}, \tag{6d}$$

$$\mu\frac{[2(w_z-u_x)h_x-(u_y+v_x)h_y-h_yh_x(v_z+w_y)+(u_z+w_x)(1-h_x^2)]}{\sqrt{1+h_x^2+h_y^2}}=\sigma_x, \tag{6e}$$

$$\mu\frac{[2(w_z-v_y)h_y-(u_y+v_x)h_x-h_yh_x(u_z+w_x)+(v_z+w_y)(1-h_y^2)]}{\sqrt{1+h_x^2+h_y^2}}=\sigma_y, \tag{6f}$$

where $\mathbf{v}=(u,v,w)$, $\mu=\nu\rho$ is the fluid viscosity, and σ_x, σ_y are the full derivatives of the surface tension $\sigma=\sigma[x,y,z=h(x,y)]$ with respect to x and y, respectively. To account for the Marangoni effect we also assume linear variation of surface tension σ with both temperature and solute concentration

$$\sigma(\vartheta,c)=\sigma_0-\sigma_t(\vartheta-\vartheta_0)+\sigma_c(c-c_0), \tag{7}$$

where $\sigma_t=-\partial\sigma/\partial\vartheta$, $\sigma_c=\partial\sigma/\partial c$, while σ_0, ϑ_0 and c_0 are, respectively, the reference values of surface tension, temperature, and concentration.

B. Base state

The base state for the temperature in the solid layer $-h_s<z<0$ satisfies the problem

$$\vec{\nabla}^2\vartheta^s=0, \tag{8a}$$

$$z=-h_s:\vartheta^s=\vartheta_-, \tag{8b}$$

$$z=0:\lambda\vartheta_z=\lambda^s\vartheta_z^s,\vartheta=\vartheta^s. \tag{8c}$$

The solution of Eqs. (8) is

$$\vartheta^s(z)=\vartheta_--\frac{\lambda a}{\lambda^s}(z+h_s), \tag{9}$$

where $a\equiv-\vartheta_z|_{z=0}$.

To find the base solution for the temperature field in the static liquid layer $0<z<h_0$, we solve

$$\vec{\nabla}^2\vartheta=0, \tag{10a}$$

$$z=0:\vartheta=\vartheta^s=\vartheta_--\frac{\lambda a h_s}{\lambda^s}, \tag{10b}$$

$$z = h_0 : \lambda \vartheta_z + q(\vartheta - \vartheta_+) = 0, \tag{10c}$$

and obtain

$$\vartheta(z) = \vartheta_- - \frac{\lambda a h_s}{\lambda^s} - az, \tag{11}$$

where the parameter a can be expressed using physical parameters of the problem as

$$a = \frac{q(\vartheta_- - \vartheta_+)}{\lambda + q\left(\frac{\lambda}{\lambda^s} h_s + h_0\right)}. \tag{12}$$

C. Nondimensional form of equations and boundary conditions

We define the dimensionless variables of the problem using the scaling

$$t \to \frac{h_0^2}{\nu} t, \quad (x,y,z) \to h_0 (x,y,z), \quad (u,v,w) \to \frac{\kappa}{h_0}(u,v,w), \tag{13a}$$

$$\vartheta \to \vartheta_+ + a h_0 T, \quad c \to \frac{\sigma_t}{\sigma_c} a h_0 C, \quad p \to \frac{\mu\kappa}{h_0^2} p. \tag{13b}$$

This yields dimensionless form of the governing equations in the liquid phase

$$\vec{\nabla} \cdot \mathbf{v} = 0, \tag{14a}$$

$$\mathbf{v}_t + P^{-1}(\mathbf{v} \cdot \vec{\nabla})\mathbf{v} = -\vec{\nabla} p + \vec{\nabla}^2 \mathbf{v} - G\mathbf{e}_z, \tag{14b}$$

$$P T_t + \mathbf{v} \cdot \vec{\nabla} T = \vec{\nabla}^2 T, \tag{14c}$$

$$S C_t + L^{-1} \mathbf{v} \cdot \vec{\nabla} C = \vec{\nabla}^2 C + \chi \vec{\nabla}^2 T, \tag{14d}$$

the heat equation in the solid phase

$$P T_t^s = \tilde{\kappa} \vec{\nabla}^2 T^s, \tag{15}$$

while the boundary conditions are recast in the form

$$z = -\tilde{h} : T^s = \Theta, \tag{16a}$$

$$z = 0 : \mathbf{v} = 0, \quad T_z = \tilde{\lambda} T_z^s, \quad T = T^s, \quad C_z = -\chi T_z, \tag{16b}$$

$$z = h(x,y,t) : \vec{\nabla} T \cdot \mathbf{n} + BT = \vec{\nabla} C \cdot \mathbf{n} - \chi BT = 0,$$

$$P h_t + u h_x + v h_y = w, \tag{16c}$$

$$\frac{1}{(1 + h_x^2 + h_y^2)^{1/2}} [2(w_z - u_x) h_x - (u_y + v_x) h_y - h_y h_x (v_z + w_y) + (u_z + w_x)(1 - h_x^2)] = M[C_x - T_x + h_x (C_z - T_z)], \tag{16d}$$

TABLE I. Dimensionless parameters of the problem and their typical experimental values for aqueous binary mixtures. Parameters depending on the control values, such as the mean layer thickness h_0 and the applied thermal gradient a are excluded. The parameters P, S, B, and χ are defined in Eq. (17), L is defined in the paragraph following Eq. (17), and b_0 is defined in Eq. (25).

Dimensionless parameter	Typical values
P	3–10
S	10^2–10^3
L	10^{-3}–3×10^{-2}
B	10^{-4}–10^{-2}
b_0	10^{-5}–10^{3}
χ	−1–1

$$\frac{1}{(1 + h_x^2 + h_y^2)^{1/2}} [2(w_z - v_y) h_y - (u_y + v_x) h_x - h_y h_x (u_z + w_x) + (v_z + w_y)(1 - h_y^2)] = M[C_y - T_y + h_y (C_z - T_z)], \tag{16e}$$

$$-p + \frac{2}{1 + h_x^2 + h_y^2} [u_x (h_x^2 - 1) + v_y (h_y^2 - 1) - h_x (u_z + w_x) + (u_y + v_x) h_x h_y - (w_y + v_z) h_y] = \Sigma \frac{h_{xx}(1 + h_y^2) + h_{yy}(1 + h_x^2) - 2 h_x h_y h_{xy}}{(1 + h_x^2 + h_y^2)^{3/2}}, \tag{16f}$$

where the dimensionless parameters of the problem

$$P = \frac{\nu}{\kappa}, \quad S = \frac{\nu}{D}, \quad \chi = \frac{\alpha \sigma_c}{\sigma_t}, \quad B = \frac{q h_0}{\lambda}, \quad M = \frac{\sigma_t a h_0^2}{\mu\kappa},$$

$$G = \frac{g h_0^3}{\nu\kappa}, \tag{17}$$

are the Prandtl, Schmidt, Soret, Biot, Marangoni, and modified Galileo numbers, respectively, and $\Sigma = \frac{\sigma h_0}{\mu\kappa}$ is the inverse capillary (or surface tension) number. It is found to be convenient to use hereafter also the Lewis number $L = P/S$. We also introduce new parameters $\tilde{\lambda} = \lambda^s/\lambda$, $\tilde{\kappa} = \kappa^s/\kappa$, that denote relative thermal conductivity and diffusivity of the solid and liquid phases, respectively, $\Theta = (\vartheta_- - \vartheta_+)/(a h_0)$ and $\tilde{h} = h_s/h_0$. It is also useful to note that the solutal Marangoni number can be expressed as $M_c = ML^{-1}\chi$. A summary of the dimensionless parameters of the problem independent of control factors is presented in Table I.

D. Linearized problem

The base state whose stability will be studied here is given by

$$\bar{\mathbf{v}} = \mathbf{0}, \quad \bar{T} = -z + \frac{1 + B}{B}, \quad \bar{T}^s = -\frac{z}{\tilde{\lambda}}\left(1 + \frac{1 + B}{B}\right),$$

$$\bar{C} = \chi z + \text{const}, \quad \bar{p} = -G(z - 1). \tag{18}$$

Because of the rotation invariance of the problem, it is sufficient to investigate the stability of the base state with respect to two-dimensional disturbances. Introducing normal perturbations $(u,w,p,T,T^s,C,\zeta)=(\tilde{u},\tilde{w},\tilde{p},\tilde{T},\tilde{T}^s,\tilde{C},\tilde{\zeta})e^{ikx+\omega t}$, where k and ω are, respectively, the dimensionless wave number and growth rate of the disturbance, yields in terms of the amplitudes of perturbation functions

$$ik\tilde{u}+\tilde{w}_z=0, \tag{19a}$$

$$\omega\tilde{u}=-ik\tilde{p}-k^2\tilde{u}+\tilde{u}_{zz}, \tag{19b}$$

$$\omega\tilde{w}=-\tilde{p}_z-k^2\tilde{w}+\tilde{w}_{zz}, \tag{19c}$$

$$\omega P\tilde{T}-\tilde{w}=-k^2\tilde{T}+\tilde{T}_{zz}, \tag{19d}$$

$$\omega PL^{-1}\tilde{C}+L^{-1}\chi\tilde{w}=-k^2\tilde{C}+\tilde{C}_{zz}+\chi(-k^2\tilde{T}+\tilde{T}_{zz}), \tag{19e}$$

where $\zeta=\zeta(x,t)$ is the deviation of the interface from its flat state $z=1$.

In the solid phase the heat equation yields

$$P\omega\tilde{T}^s=\tilde{\kappa}(-k^2\tilde{T}^s+\tilde{T}^s_{zz}). \tag{19f}$$

The boundary conditions now become, at $z=-\tilde{h}$,

$$\tilde{T}^s=0 \tag{19g}$$

at $z=0$

$$\tilde{u}=\tilde{w}=0, \quad \tilde{T}=\tilde{T}^s, \quad \tilde{T}_z=\tilde{\lambda}\tilde{T}^s_z, \quad \tilde{C}_z=-\chi\tilde{T}_z, \tag{19h}$$

at $z=1$

$$\tilde{T}_z+B(\tilde{T}-\tilde{\zeta})=0, \tag{19i}$$

$$\tilde{C}_z-\chi B(\tilde{T}-\tilde{\zeta})=0, \tag{19j}$$

$$\omega P\tilde{\zeta}=\tilde{w}, \tag{19k}$$

$$G\tilde{\zeta}-\tilde{p}-2ik\tilde{u}=-k^2\tilde{\zeta}\Sigma, \tag{19l}$$

$$\tilde{u}_z+ik\tilde{w}=ikM[\tilde{C}-\tilde{T}+\tilde{\zeta}(\chi+1)]. \tag{19m}$$

Solving Eq. (19f) with boundary conditions (19g) and (19h), yields the relation between the perturbation of the temperature and its vertical derivative at the solid-liquid interface $z=0$

$$\tilde{T}_z(0)=b(k^2,\omega)\tilde{T}(0), \tag{20}$$

where

$$b(k^2,\omega)=\tilde{\lambda}\sqrt{\frac{P\omega}{\tilde{\kappa}}+k^2}\coth\left\{\sqrt{\frac{P\omega}{\tilde{\kappa}}+k^2}\tilde{h}\right\} \tag{21}$$

represents the Biot number at the solid-liquid interface. The expression (20) will be used below as the boundary condition for the perturbation of the liquid temperature at the rigid bottom plane $z=0$. The long-wave case and the case of finite wave numbers will be now studied separately.

III. LINEAR STABILITY THEORY

In contrast with our previous papers [14,15], here we deal with the case of finite Biot numbers at both solid-liquid and liquid-gas interfaces. The case of a system with both poorly conducting boundaries was considered in Ref. [14], while in Ref. [15] the heat transfer was characterized by the Biot number of a unity order at the upper free deformable liquid-gas surface and a specified heat flux at the rigid bottom surface corresponding to a zero effective Biot number in terms of disturbances at the solid-liquid interface. From the experimental point of view, it is practically impossible to set up a system with poorly conducting boundaries with prescribed heat fluxes there, therefore our present analysis with finite Biot numbers relaxes that assumption and seems to be less restrictive from the physical point of view.

In real physical problems the Lewis number L is small, i.e., $L\sim O(10^{-4}-10^{-2})$, e.g., in ^{3}He-^{4}He mixtures $L=0.04$ [16], in water-ethanol mixtures $L=0.02$ at room temperature [16], and in magnetic colloidal mixtures [17], $L=1.2\times10^{-4}$. Thus, it becomes quite natural to consider the long-wave Marangoni instability in the case of a small Lewis number. The choice of our scaling here is based on the results of analysis that was carried out in our previous paper [15]. There, we showed that the long-wave oscillatory instability emerges if the condition $G<45L$ is satisfied. Hence, we expect that in the limit of a small Lewis number and a unity-order Galileo number, the oscillatory instability never sets in. It was also shown [15] that the most important case when both long-wave monotonic and oscillatory instability emerge, is the limit of both small L and G.

As will be shown below, the scaling of a characteristic wave number of the disturbance is determined by the order of magnitude of a small Lewis number and three distinguished asymptotic limits emerge: (i) a long-wave limit $k=O(L^{1/2})$ whose scaling is explained in Ref. [15]; (ii) the case of finite wave numbers $k=O(1)$; (iii) an intermediate asymptotics of the long-wave monotonic instability $k=O(L^{1/4})$.

A. The case $k=O(\varepsilon)$

It is convenient to introduce a small scaling parameter ε in such a way that $L=\varepsilon^2 l$, $G=\varepsilon^2 g$, $l=O(1)$, $g=O(1)$. In the region $k=O(L^{1/2})$ we have $k=\varepsilon K$, $K=O(1)$. As it was shown in Ref. [15], the Marangoni number and the growth rate of the disturbance are expanded as

$$M=\varepsilon^2(M_0+\varepsilon^2M_2+\cdots), \quad \omega=\varepsilon^4(\omega_0+\varepsilon^2\omega_2+\cdots), \tag{22}$$

where M_0 is the critical value of the Marangoni number and ε is a small scaling parameter serving as a measure of smallness of the disturbance wave number. The amplitudes of the perturbation functions are expanded in the form

$$(\tilde{\zeta},\tilde{T},\tilde{C},\tilde{p}) = (\zeta_0,T_0,C_0,p_0) + \varepsilon^2(\zeta_2,T_2,C_2,p_2) + \cdots,$$

$$\tilde{u} = \varepsilon(u_0 + \varepsilon^2 u_2 + \cdots), \quad \tilde{w} = \varepsilon^2(w_0 + \varepsilon^2 w_2 + \cdots). \tag{23}$$

The lower Biot number b found in Eq. (21) is also expanded in the form

$$b(K^2) = b_0 + \varepsilon^2 b_2(K^2) + O(\varepsilon^4), \tag{24}$$

where

$$b_0 = \frac{\tilde{\lambda}}{\tilde{h}}, \quad b_2 = \frac{\tilde{\lambda}\tilde{h}K^2}{3}. \tag{25}$$

All these are substituted into Eqs. (19). At zero order the solution is given by

$$T_0 = \frac{B(1+b_0 z)\zeta_0}{b_0 + B + b_0 B}, \quad C_0 = a_0 - \frac{b_0 B z \chi \zeta_0}{b_0 + B + b_0 B}, \tag{26a}$$

$$p_0 = 0, \quad u_0 = 0, \quad w_0 = 0, \tag{26b}$$

where a_0 is constant yet to be determined.

At second order the problem reads

$$iKu_2 + w_{2,z} = 0, \tag{27a}$$

$$-iKp_2 - K^2 u_0 + u_{2,zz} = 0, \tag{27b}$$

$$-p_{2,z} + w_{0,zz} = 0, \tag{27c}$$

$$-w_0 = -K^2 T_0 + T_{2,zz}, \tag{27d}$$

$$-K^2 C_0 + C_{2,zz} - \chi K^2 T_0 + \chi T_{2,zz} = l^{-1}\chi w_2 + P l^{-1}\omega_0 C_0, \tag{27e}$$

$$z = 0: u_2 = w_2 = 0, \quad T_{2,z} = b_0 T_2 + b_2 T_0,$$

$$C_{2,z} = -\chi(b_0 T_2 + b_2 T_0), \tag{27f}$$

$$z = 1: T_{2,z} + B(T_2 - \zeta_2) = 0, \tag{27g}$$

$$C_{2,z} - \chi B(T_2 - \zeta_2) = 0, \tag{27h}$$

$$P\omega_0\zeta_0 = w_2, \tag{27i}$$

$$g\zeta_0 - p_2 - 2iKu_0 = -K^2\zeta_0\Sigma, \tag{27j}$$

$$u_{2,z} + iKw_0 = iKM_0\{C_0 - T_0 + \zeta_0(1+\chi)\}. \tag{27k}$$

Solving Eqs. (27) for the unknown constant a_0, we find that

$$a_0 = -\frac{\zeta_0\{3[b_0 + (b_0+B)\chi]M_0/[b_0 + B + b_0 B] - 2(g + K^2\Sigma + 3P\Lambda_0)\}}{3M_0}, \tag{28}$$

where $\Lambda_0 = K^{-2}\omega_0$.

Integrating Eqs. (27d) and (27e) across the layer and taking into account the boundary conditions (27f)–(27h) for the temperature and solute concentration perturbations, we obtain the dispersion relation at second order in the form

$$16(l + P\Lambda_0)(g + K^2\Sigma + 3P\Lambda_0) - \frac{1}{3[B + b_0(1+B)]} \times [M_0(B(g + K^2\Sigma + 48P\Lambda_0)\chi + \{(1+B)K^2\Sigma\chi + 12P\Lambda_0[6 + (4+B)\chi] + [(1+B)g\chi + 72l(1+\chi)]\}b_0)] = 0. \tag{29}$$

Solving Eq. (29) yields two modes of the growth rate

$$\Lambda_\pm = -\frac{1}{24P[B + b_0(1+B)]}(4B(g + 3l + K^2\Sigma - M_0\chi) - \{-4(1+B)(g + 3l + K^2\Sigma) + M_0[6 + (4+B)\chi]\}b_0 \pm \sqrt{R}), \tag{30}$$

where

$$R = 16(g - 3l + K^2\Sigma)^2[B + (1+B)b_0]^2 + M_0^2\{4B\chi + [6 + (4+B)\chi]b_0\}^2 - 4M_0[B + (1+B)b_0](B(7g + 24l + 7K^2\Sigma)\chi + \{6l[-6 + (-8+B)\chi] + g[12 + (7+B)\chi] + K^2\Sigma[12 + (7+B)\chi]\}b_0). \tag{31}$$

In the limit of a large wave number, $K^2 \gg 1$, the asymptotic behavior of these two modes of Eq. (30) is

$$\Lambda_- = O(K^2) = -\frac{K^2\Sigma}{3P}, \tag{32a}$$

$$\Lambda_+ = O(1) = \frac{1}{48}(-48l + M_0\chi). \tag{32b}$$

Thus, the first mode, Eq. (32a) is always stable in the short-wave domain, while the second one, Eq. (32b) is stable under condition $M_0\chi < 48l$.

1. Monotonic instability

Assuming $\Lambda_0 = 0$ in Eq. (29), we obtain at leading order the monotonic instability threshold

$$M_0 = \frac{48(b_0 + B + b_0 B) l (g + K^2 \Sigma)}{B(g + K^2\Sigma)\chi + b_0[(1+B)(g+K^2\Sigma)\chi + 72l(1+\chi)]}. \tag{33}$$

From Eq. (33) for the threshold of monotonic instability, one can make the following conclusions. If $\chi(1+\chi)>0$, the minimum of the monotonic neutral curve is located in the long-wave region and

$$M_0 = M_0(K=0) = \frac{48(b_0 + B + b_0 B) g l}{Bg\chi + b_0[(1+B)g\chi + 72l(1+\chi)]}. \tag{34}$$

If $\chi(1+\chi)<0$, two different cases are possible:

(i) If $g < -\frac{72 b_0 (1+\chi) l}{B + b_0 (1+B)\chi}$, the monotonic neutral curve is discontinuous at

$$K^2 = K_*^2 = -\frac{Bg\chi + b_0[(1+B)g\chi + 72l(1+\chi)]}{(b_0 + B + b_0 B)\Sigma\chi}. \tag{35}$$

In this case in the domain $K<K_*$, the minimum of the monotonic neutral curve is attained at $K=0$, i.e., the instability is long wave. There might be an additional minimum of the monotonic neutral curve in the domain $K>K_*$ located outside the region $k=O(\varepsilon)$. The present theory is unable to investigate instability in the domain of finite wave numbers. This issue will be addressed and the analysis will be continued in the next section.

(ii) If $g > -\frac{72 b_0 (1+\chi) l}{B + b_0 (1+B)\chi}$, the monotonic neutral curve is continuous and its minimal value is attained outside the region $k=O(\varepsilon)$.

2. Oscillatory instability

Assuming $\Lambda_0 = i\Omega_0$, where Ω_0 is real in Eq. (29) and separating out the real and imaginary parts, we obtain at leading order the expressions for both oscillatory instability threshold and the corresponding squared frequency

$$M_{\rm osc} = \frac{4(b_0 + B + b_0 B)(g + 3l + K^2\Sigma)}{4B\chi + b_0[6 + (4+B)\chi]}, \tag{36}$$

$$\Omega_0^2 = -\frac{\chi(g+K^2\Sigma)[B(g - 45l + K^2\Sigma) + b_0(1+B)(g+K^2\Sigma) - 9b_0 l(B-3)] + 216 b_0 l^2 (1+\chi)}{36P^2\{4B\chi + b_0[6+(4+B)\chi]\}}. \tag{37}$$

3. Competition of monotonic and oscillatory modes of instability

We now address the question of what type of instability sets in first in various regions of parameters B, b_0 and χ. We find that Eq. (36) changes its sign at

$$\chi = \chi_{\rm osc} = -\frac{6 b_0}{4B + b_0(4+B)}, \tag{38}$$

while $1+\chi_{\rm osc}$ changes its sign at

$$b_0^{(\rm osc)} = \frac{-4B}{B-2}. \tag{39}$$

Introducing a new variable being an associated squared wave number $\tilde{g} = g + K^2\Sigma$, we find that in the domain $-1<\chi<0$, the expression for the monotonic instability curve (33) becomes discontinuous and changes its sign at the point

$$\tilde{g}_0 = -\frac{72 b_0 l (1+\chi)}{(b_0 + B + b_0 B)\chi}. \tag{40}$$

We also find that the intersection of the monotonic and oscillatory neutral curves takes place at the points

$$\tilde{g}_{1,2} = \frac{9[b_0(-3+B) + 5B] l\chi \mp 3\sqrt{3} l \sqrt{Q}}{2(b_0 + B + b_0 B)\chi}, \tag{41}$$

where

$$Q = \chi\{3[b_0(-3+B) + 5B]^2\chi - 32 b_0 (b_0 + B + b_0 B)(1+\chi)\}. \tag{42}$$

Both expressions (41) are discontinuous at $\chi=0$. In addition, if $B>3$ then $\tilde{g}_2(\chi=-1)=0$ for all b_0; if $B>3$ then for $b_0 < b_0^*$, $\tilde{g}_2(\chi=-1)=0$ and for $b_0 > b_0^*$, $\tilde{g}_1(\chi=-1)=0$, where

$$b_0^* = -\frac{5B}{B-3}. \tag{43}$$

The expression (42) vanishes at

$$\chi = 0 \quad \text{and} \tag{44}$$

$$\chi = \chi_* = \frac{32 b_0 (b_0 + B + b_0 B)}{-5b_0^2 - 2b_0(61 + 25 b_0)B + 3(5+b_0)^2 B^2}. \tag{44}$$

The last expression χ_* changes its sign through infinity at

$$b_0^{(1)} = \frac{B(61 - 15B - 8\sqrt{64 + 30B})}{-5 + B(-50 + 3B)}. \tag{45}$$

It should be noted that $b_0^{(1)}>0$ for $B<16.7661$, i.e., for all realistic values of the Biot number at the gas-liquid interface.

The value χ_* merges with $\chi_{\rm osc}$ at the point

$$b_0^{(0)} = \frac{17B}{7 - 5B}. \tag{46}$$

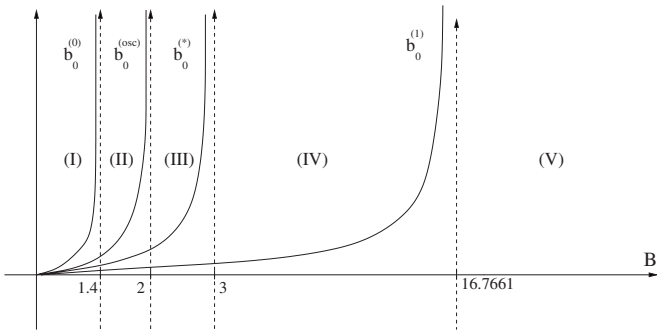

FIG. 2. Five regions of parameter B, where depending on the values of B, b, and χ the competition between long-wave monotonic and oscillatory modes of instability takes place following one of the eight types of scenarios, as shown in Figs. 3(a)–3(g).

Our analysis shows that there exist five regions of parameter B, as shown in Fig. 2, where depending on values of B, b, and χ, the competition between monotonic and oscillatory modes of instability takes place according to one of the eight possible scenarios presented in Fig. 3. In regions I and II, $\chi_* < \chi_{osc} < -1$ and for $\chi \leqslant \chi_{osc}$, the marginal curve is as in (f)-lower curve; for $\chi_{osc} < \chi \leqslant -1$, the marginal curve is as in (g); for $-1 < \chi < 0$, the marginal curve is as in (e); for $\chi \geqslant 0$, the marginal curve is as in (f)-upper curve. In regions III and IV, $\chi_* < -1 < \chi_{osc} < 0$ and for $\chi \leqslant \chi_*$, the marginal curve is as in (f)-lower curve; for $\chi_* < \chi < -1$, the marginal curve is as in (f)-lower curve in III and (a_) in IV; for $\chi = -1$, the marginal curve is as in (b); for $-1 < \chi < \chi_{osc}$, the marginal curve is as in (c); for $\chi = \chi_{osc}$, the marginal curve is as in (d); for $\chi_{osc} < \chi < 0$, the marginal curve is as in (e); for

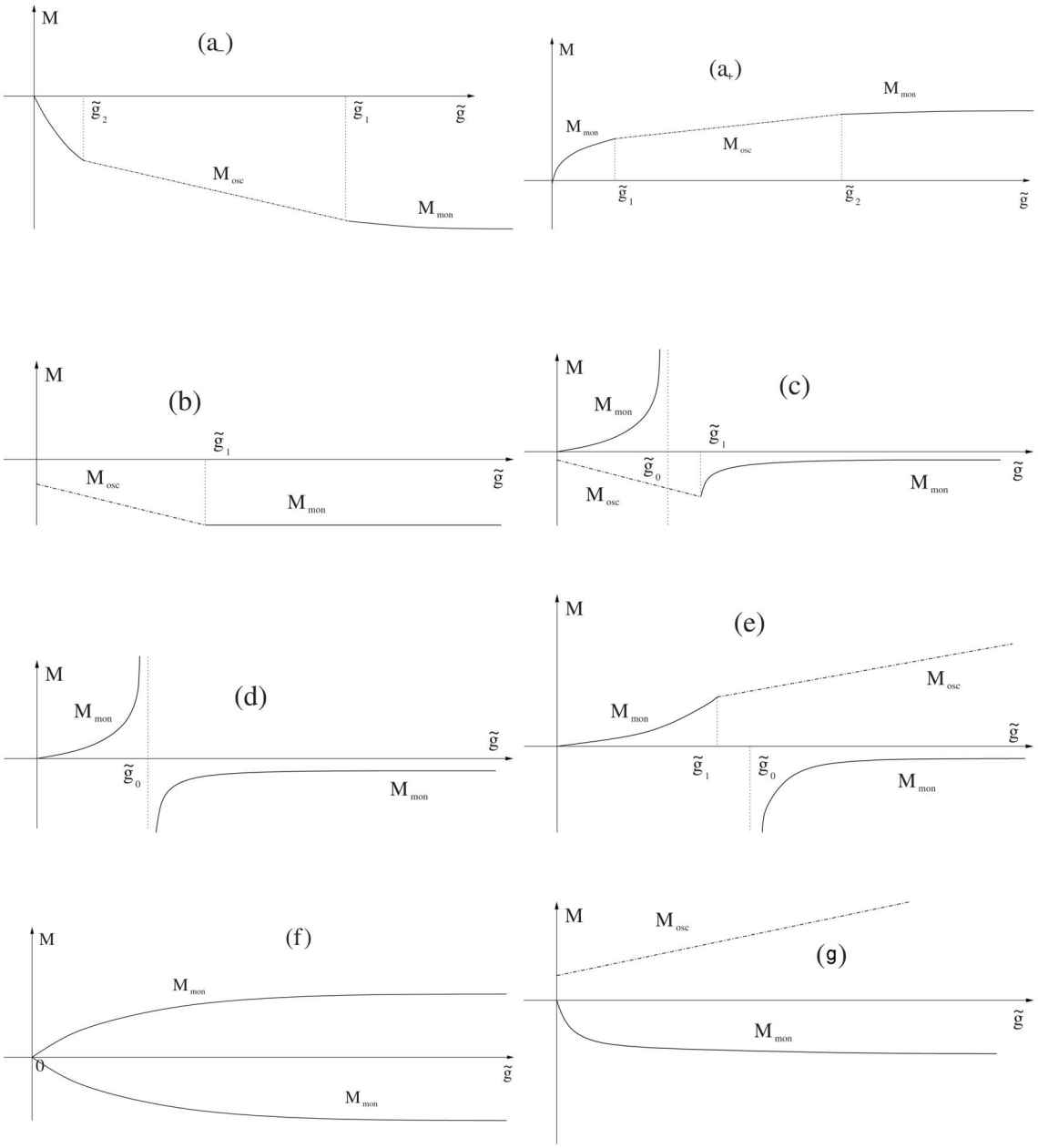

FIG. 3. Typical shapes of the neutral curves in the case of the long-wave instability for $k = O(\varepsilon)$ shown in the $\tilde{g}$-M plane.

$\chi \geqslant 0$, the marginal curve is as in (f)-upper curve. In region V, $-1 < \chi_{osc} < 0 < \chi_*$ and for $\chi < -1$, the marginal curve is as in (a_-); for $\chi = -1$, the marginal curve is as in (b); for $-1 < \chi < \chi_{osc}$, the marginal curve is as in (c); for $\chi = \chi_{osc}$, the marginal curve is as in (d); for $\chi_{osc} < \chi < 0$, the marginal curve is as in (e); for $0 \leqslant \chi \leqslant \chi_*$, the marginal curve is as in (f)-upper curve; for $\chi > \chi_*$, the marginal curve is as in (a_+).

In conclusion to this subsection, we compare between the present results and those of our previous investigations [14,15]. Observing the expressions derived for the thresholds of monotonic, Eq. (33), and oscillatory, Eq. (36), instabilities, which contain both Biot numbers and the Lewis number, one can see that *both* thermocapillarity and solutocapillarity are equally important for the development of instability. This circumstance is clear from the structure of the eigenfunctions: the disturbances T_0 and C_0 are of the same order of magnitude, see Eq. (26a). In contrast with this, for a system with poorly conducting boundaries, the contribution of thermocapillarity, as compared to that of solutocapillarity, to the interfacial shear stress rapidly decreases with a decrease of the wave number of the disturbance when $k = O(B^{1/2})$ [14]. Therefore, the instability threshold is presented in terms of the solutal Marangoni number and is independent of the Biot number. One more essential difference of the present research from our paper [14] is a treatment of the case of small Lewis and Galileo numbers. In Ref. [14], we considered the limit when Lewis and Galileo numbers are small, but much larger than the disturbance wave number for the system with poorly conducting boundaries in the long-wave domain $k = O(B^{1/2})$. At leading order we obtain that the marginal monotonic curve is in the range $O(L)$, while the oscillatory curves are in the domain $O(1)$. Therefore, the oscillatory instability can be more dangerous only when the critical Marangoni number for the oscillatory instability differs in sign with that of the critical value of the Marangoni number for the monotonic instability. In the present paper, in the limit of $L, G = O(\varepsilon^2) \ll k = O(\varepsilon)$, our results show that both oscillatory and monotonic instability curves lie in the similar asymptotic domains and depending on the values of the Biot and Soret numbers, either of the two types of instability can set in.

A qualitative clear-cut distinction between the results obtained here and those of the linear long-wave stability theory in the limit of both asymptotically small Lewis and Galileo numbers [15], has to be made now. In the present case of the long-wave instability for both finite Biot numbers, a variety of different scenarios presented in Fig. 3 emerges. However, in the case of a low-conductivity solid substrate [15], the minimum of the oscillatory neutral curve is always located at $K = 0$, as shown in Fig. 3(b), i.e., only one specific case (b) materializes.

B. The case $k = O(1)$

As shown above, the analysis carried out with $k = O(\varepsilon)$ is not sufficient for finding the minimum of the monotonic neutral curve in the case when $-1 < \chi < 0$. Therefore, it is necessary to analyze the case $k \gg \varepsilon$. First, consider the monotonic instability under assumption $k = O(1)$. We obtain the following problem for the perturbation functions:

$$ik\tilde{u} + \tilde{w}_z = 0, \tag{47a}$$

$$-ik\tilde{p} - k^2\tilde{u} + \tilde{u}_{zz} = 0, \tag{47b}$$

$$-\tilde{p}_z - k^2\tilde{w} + \tilde{w}_{zz} = 0, \tag{47c}$$

$$-\tilde{w} = -k^2\tilde{T} + \tilde{T}_{zz}, \tag{47d}$$

$$L^{-1}\chi\tilde{w} = -k^2\tilde{C} + \tilde{C}_{zz} + \chi(-k^2\tilde{T} + \tilde{T}_{zz}), \tag{47e}$$

at $z = 0$

$$\tilde{u} = \tilde{w} = 0, \quad \tilde{T}_z = b(k^2)\tilde{T}, \quad \tilde{C}_z = -\chi\tilde{T}_z, \tag{47f}$$

at $z = 1$

$$\tilde{T}_z + B(\tilde{T} - \tilde{\zeta}) = 0, \tag{47g}$$

$$\tilde{C}_z - \chi B(\tilde{T} - \tilde{\zeta}) = 0, \tag{47h}$$

$$\tilde{w} = 0, \tag{47i}$$

$$G\tilde{\zeta} - \tilde{p} - 2ik\tilde{u} = -k^2\tilde{\zeta}\Sigma, \tag{47j}$$

$$\tilde{u}_z + ik\tilde{w} = ikM[\tilde{C} - \tilde{T} + \tilde{\zeta}(\chi + 1)], \tag{47k}$$

where $b(k^2)$ is given by Eq. (21).

Following scaling for the parameters and the variables of the problem is applied:

$$L = \varepsilon^2 l, \quad G = \varepsilon^2 g, \quad M = \varepsilon^2(M_0 + \varepsilon^2 M_2 + \cdots), \tag{48}$$

$$(\tilde{\zeta}, \tilde{T}, \tilde{C}, \tilde{p}, \tilde{u}, \tilde{w}) = (\zeta_0, T_0, C_0, p_0, u_0, w_0) + \varepsilon^2(\zeta_2, T_2, C_2, p_2, u_2, w_2) + \cdots . \tag{49}$$

It should be noted that at the leading order, the thermal disturbance T_0 vanishes, whereas the solutal disturbance C_0 does not. Using (49) we obtain at leading order for the threshold of the monotonic instability in the domain $k = O(1)$

$$M_0 = \frac{16k^2 l[k - \cosh(k)\sinh(k)]}{2k\chi[2 + k^2 - k\coth(k)] - \chi\sinh(2k)}. \tag{50}$$

This result can be presented in terms of the solutal Marangoni number $M_s \equiv M\chi L^{-1}$, and it is independent of the Biot numbers. That is because in the region of finite wave numbers the convection is caused solely by the solutocapillary effect.

The analysis of Eq. (50) shows that the minimal value is attained at $k = 0$ and there are no additional minima of the neutral curve in the region of finite wave numbers $k = O(1)$. Hence, in the case $-1 < \chi < 0$, the minimum is located in the region $\varepsilon \ll k \ll 1$.

C. Intermediate asymptotics of the long-wave monotonic instability for $k = O(\sqrt{\varepsilon})$

In order to match the results obtained in the regions $k = O(\varepsilon)$ and $k = O(1)$, it is necessary to consider the interme-

diate region of wave numbers. To determine the characteristic scale of the matching region, we first analyze the asymptotics of the obtained fragments of the neutral curve.

It is easy to see that the threshold of the monotonic instability in the long-wave region $k=\varepsilon K$, Eq. (33), can be rewritten in the form

$$M_0 = \tilde{M}\frac{1+\frac{g}{\Sigma}K^{-2}}{1+\alpha K^{-2}}, \tag{51}$$

where

$$\tilde{M} = \frac{48l}{\chi}, \quad \alpha = \frac{Bg\chi + (1+B)g\chi b_0 + 72l(1+\chi)b_0}{\Sigma\chi[B+(1+B)b_0]}. \tag{52}$$

In the limit of large wave numbers K we obtain at leading order

$$M_0 = \tilde{M}\left[1+\left(\frac{g}{\Sigma}-\alpha\right)K^{-2}\right] + O(K^{-4}) = \frac{48l}{\chi} - \frac{3456l^2(1+\chi)b_0}{K^2\Sigma\chi^2(B+b_0+Bb_0)} + O(K^{-4}). \tag{53}$$

Hence, taking into account our scaling in this limit ($k=\varepsilon K$, $L=\varepsilon^2 l$), one obtains

$$M = \varepsilon^2[M_0 + O(\varepsilon^2)] = \frac{48L}{\chi} - \frac{3456L^2(1+\chi)b_0}{k^2\Sigma\chi^2(B+b_0+Bb_0)} + O(\varepsilon^4). \tag{54}$$

Thus, investigating the asymptotic behavior of Eq. (51) in the limit of large wave numbers K, results in the following cases.

(1) $\alpha > \frac{g}{\Sigma} > 0$: In this case the neutral curve is monotonically increasing, as shown in Fig. 4 (upper panel).

(2) $0 < \alpha < \frac{g}{\Sigma}$: In this case the neutral curve has a minimum in the region of large K, as shown in Fig. 4 (middle panel).

(3) $\alpha < 0$: In this case, as in the previous one, the neutral curve has a minimum in the region of large K, as shown in Fig. 4 (lower panel).

Investigating the asymptotic behavior of the threshold of the monotonic instability in the region of finite wave numbers (50), in the limit of small k at leading order, we obtain

$$M = \varepsilon^2[M_0 + O(\varepsilon^2)] = \frac{48L}{\chi} + \frac{16k^2L}{5\chi} + O(k^3). \tag{55}$$

We can expect that matching the expressions given by Eqs. (54) and (55) can be achieved when

$$L^2/k^2 \sim k^2 L, \quad \text{i.e., } k = O(L^{1/4}) = O(\varepsilon^{1/2}).$$

The corresponding intermediate region of k has to be considered in more detail.

Based on the arguments presented above, we choose the following scaling for the parameters of the problem in the linear system for perturbation functions (19a)–(19e) with boundary conditions (19h)–(19m) and (20)

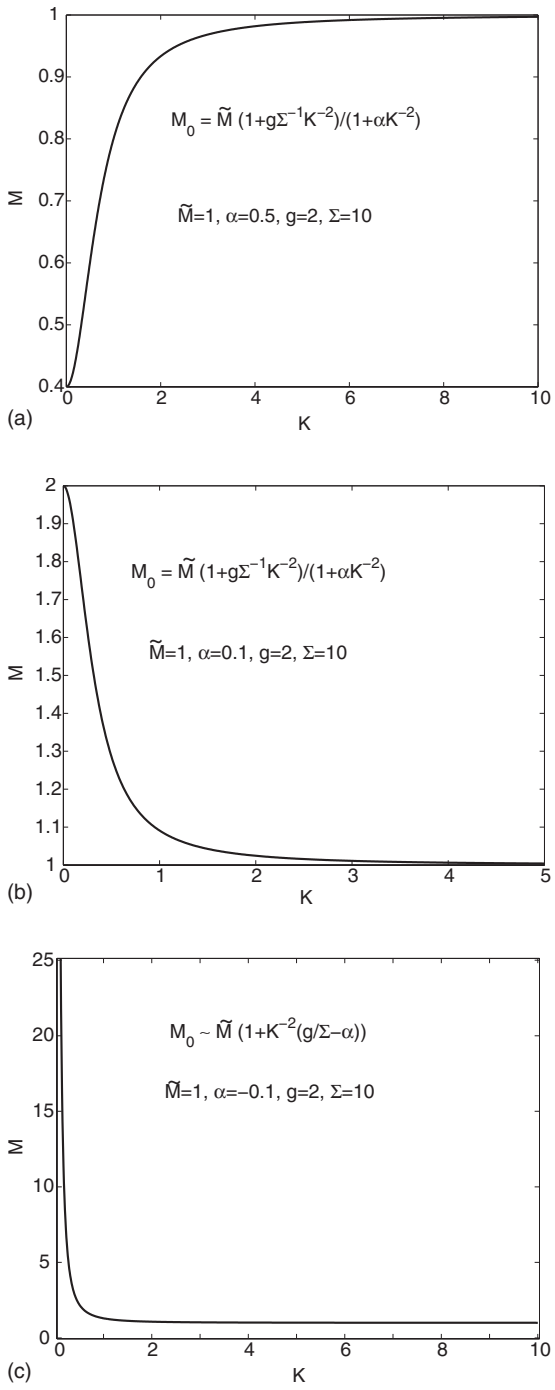

FIG. 4. Asymptotic behavior of the critical Marangoni number for the long-wave monotonic instability given by Eq. (51) in the limit of large wave numbers K for (upper panel) $\alpha > \frac{g}{\Sigma} > 0$, where $\tilde{M}$ and α are given by Eq. (52). $\tilde{M}=1$, $\alpha=0.5$, $g=2$, and $\Sigma=10$, (Middle panel) $0<\alpha<\frac{g}{\Sigma}$, $\tilde{M}=1$, $\alpha=0.1$, $g=2$, and $\Sigma=10$. (Lower panel) $\alpha<0$, $\tilde{M}=1$, $\alpha=-0.1$, $g=2$, and $\Sigma=10$.

$$k = \sqrt{\varepsilon}K, \quad L = \varepsilon^2 l, \quad G = \varepsilon^2 g, \tag{56a}$$

$$M = \varepsilon^2(M_0 + \varepsilon M_1 + \cdots), \tag{56b}$$

$$b = b_0 + \varepsilon b_1 + \cdots, \tag{56c}$$

$$\tilde{u} = \sqrt{\varepsilon}(u_0 + \varepsilon u_1 + \cdots), \quad \tilde{w} = \varepsilon(w_0 + \varepsilon w_1 + \cdots), \tag{56d}$$

$$(\tilde{\zeta}, \tilde{T}, \tilde{C}, \tilde{p}) = (\zeta_0, T_0, C_0, p_0) + \varepsilon(\zeta_1, T_1, C_1, p_1) + \cdots . \tag{56e}$$

Solving the obtained set of equations along with the boundary conditions at each order, we find that at zero order, the solution is given by

$$u_0 = w_0 = 0, \quad p_0 = 0, \quad T_0 = 0, \quad \zeta_0 = 0, \quad C_0 = \frac{K^2 \Sigma \chi \zeta_1}{72l}. \tag{57a}$$

At first order the solution of the problem is

$$u_1 = w_1 = 0, \quad p_1 = 0, \quad T_1 = \frac{B(1 + zb_0)\zeta_1}{B + (1 + B)b_0}, \tag{57b}$$

$$\begin{aligned} C_1 = \frac{1}{2160l[B + (1 + B)b_0]}(\chi\{[B(30g - 2160l \\ + K^4\Sigma\{1 + 3z^2[5 + 2z^2(-5 + 3z)]\}) + (30(1 + B)g \\ - 2160Blz + (1 + B)K^4\Sigma\{1 + 3z^2[5 + 2z^2(-5 \\ + 3z)]\})b_0]\zeta_1 + 30K^2\Sigma[B + (1 + B)b_0]\zeta_2\}). \end{aligned} \tag{57c}$$

Taking into account the solutions obtained above, at second order the problem becomes

$$iKu_2 + w_{2,z} = 0, \tag{58a}$$

$$-iKp_2 + u_{2,zz} = 0, \tag{58b}$$

$$-p_{2,z} = 0, \tag{58c}$$

$$-K^2T_1 + T_{2,zz} = 0, \tag{58d}$$

$$l^{-1}\chi w_3 = -K^2C_1 + C_{2,zz} - \chi K^2T_1 + \chi T_{2,zz}, \tag{58e}$$

$$z = 0: u_2 = w_2 = 0, \quad T_2 = b_1T_1 + b_0T_2, \quad C_{2,z} + \chi T_{2,z} = 0, \tag{58f}$$

$$z = 1: T_{2,z} + B(T_2 - \zeta_2) = 0, \quad C_{2,z} - \chi B(T_2 - \zeta_2) = 0, \tag{58g}$$

$$w_2 = 0, \quad p_2 = K^2\Sigma\zeta_1, \quad u_{2,z} = iKM_0C_0. \tag{58h}$$

Solving Eqs. (58a)–(58e) along with Eqs. (58f)–(58h) yields

$$u_2 = \frac{i}{6}K^3\Sigma z(-2 + 3z)\zeta_1, \tag{59a}$$

$$w_2 = \frac{1}{6}K^4\Sigma(-1 + z)z^2\zeta_1, \tag{59b}$$

$$p_2 = K^2\Sigma\zeta_1, \tag{59c}$$

$$\begin{aligned} T_2 = \frac{1}{6(B + (1 + B)b_0)^2}(B\{[K^2(-6 + 3B(-1 + z^2) \\ + b_0\{3[-1 + (-2 + z)z] + B(-1 + z)[1 + z(4 + z)] \\ + z[-3 + z^2 + B(-1 + z^2)]b_0\}) + 6[-1 + B(-1 \\ + z)]b_1]\zeta_1 + 6[B + (1 + B)b_0](1 + zb_0)\zeta_2\}). \end{aligned} \tag{59d}$$

Also, at this order of approximation we finally derive the value for the threshold of the monotonic instability in the long-wave domain $k = O(\sqrt{\varepsilon})$

$$M_0 = \frac{48l}{\chi}. \tag{60}$$

At third order we obtain the problem

$$iKu_3 + w_{3,z} = 0, \tag{61a}$$

$$-iKp_3 - K^2u_2 + u_{3,zz} = 0, \tag{61b}$$

$$-p_{3,z} + w_{2,zz} = 0, \tag{61c}$$

$$-K^2T_2 + T_{3,zz} = -w_2, \tag{61d}$$

$$l^{-1}\chi w_4 = -K^2C_2 + C_{3,zz} - \chi K^2T_2 + \chi T_{3,zz}, \tag{61e}$$

$$z = 0: u_3 = w_3 = 0, \quad T_3 = b_0T_3 + b_1T_2 + b_2T_1,$$

$$C_{3,z} + \chi T_{3,z} = 0, \tag{61f}$$

$$z = 1: T_{3,z} + B(T_3 - \zeta_3) = 0, \quad C_{3,z} - \chi B(T_3 - \zeta_3) = 0, w_3 = 0, \tag{61g}$$

$$g\zeta_1 - p_3 - 2iKu_2 = -K^2\Sigma\zeta_2, \tag{61h}$$

$$u_{3,z} + iKw_2 = iKM_0[C_1 - T_1 + \zeta_1(\chi + 1)] + iKM_1C_0. \tag{61i}$$

Solving Eqs. (61a)–(61i) results in

$$\begin{aligned} u_3 = \frac{iKz}{180}[(30g(3z - 2) + K^4\Sigma\{-6 + 5z[3 + z(3z - 4)]\})\zeta_1 \\ + 30K^2\Sigma(3z - 2)\zeta_2], \end{aligned} \tag{62a}$$

$$\begin{aligned} w_3 = \frac{K^2}{180}[(z - 1)z^2(\{30g + K^4\Sigma[3 + z(3z - 2)]\}\zeta_1 \\ + 30K^2\Sigma\zeta_2)], \end{aligned} \tag{62b}$$

$$p_3 = \frac{1}{6}(\{6g + K^4\Sigma[1 + z(3z - 2)]\}\zeta_1 + K^2\Sigma\zeta_2). \tag{62c}$$

Using the boundary condition (61i), for the first-order correction to the long-wave monotonic instability threshold in the limit $k = O(\sqrt{\varepsilon})$, we obtain

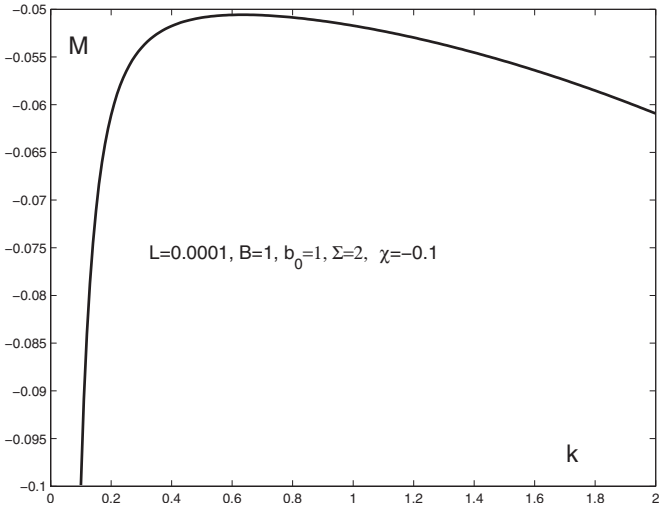

FIG. 5. The full monotonic neutral curve given by Eq. (65) in the intermediate domain $k=O(\sqrt{\varepsilon})$ for $-1<\chi<0$. This neutral curve (65) attains a minimum of the absolute value of M at the wave number determined by Eq. (66). The parameter values are $L=0.0001$, $B=1$, $b_0=1$, $\Sigma=2$, and $\chi=-0.1$.

$$M_1 = \frac{16l\{BK^4\Sigma\chi + [(1+B)K^4\Sigma\chi - 1080l(1+\chi)]b_0\}}{5K^2\Sigma\chi^2[B+(1+B)b_0]}. \tag{63}$$

It it readily seen that Eq. (63) can be recast in the form

$$M_1 = \frac{16K^2l}{5\chi} - \frac{3456l^2(1+\chi)b_0}{K^2\Sigma\chi^2(B+b_0+Bb_0)}, \tag{64}$$

and the full monotonic neutral curve is represented by

$$M = \varepsilon^2(M_0 + \varepsilon M_1 + \cdots) = \frac{48L}{\chi} + \frac{16k^2L}{5\chi} - \frac{3456L^2(1+\chi)b_0}{k^2\Sigma\chi^2(B+b_0+Bb_0)}, \tag{65}$$

where $L=\varepsilon^2 l$, $k=\sqrt{\varepsilon}K$.

Thus, when the wave number k is sufficiently small, the second term of Eq. (65) can be omitted and the result reproduces the long-wave instability threshold (54). In the same way, for sufficiently large values of the wave numbers, at leading order the third term of Eq. (65) is negligible and the two first terms are dominant. Therefore, we obtain matching with the limit of finite k, Eq. (55).

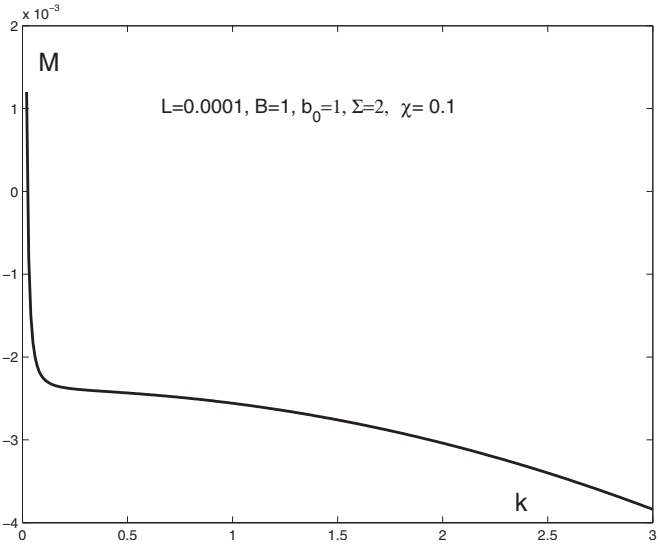

FIG. 6. The full monotonic neutral curve given by Eq. (65) in the intermediate domain $k=O(\sqrt{\varepsilon})$ for $\chi<-1$ or $\chi>0$. This neutral curve is monotonic for all k and the monotonic instability sets in at $k=0$. The parameter values are $L=0.0001$, $B=1$, $b_0=1$, $\Sigma=2$, and $\chi=0.1$.

Seeking for the minimum of the full monotonic neutral curve Eq. (65) in the intermediate domain $k=O(\sqrt{\varepsilon})$, we find that its behavior is determined by the value of the Soret number χ and the following cases are relevant:

(1) For $-1<\chi<0$, the monotonic neutral curve (65) has a minimum at

$$k_* = \left[\frac{-1080L(1+\chi)b_0}{\Sigma\chi[B+(1+B)b_0]}\right]^{1/4}, \tag{66}$$

as shown in Fig. 5.

(2) For $\chi<-1$ or $\chi>0$, the neutral curve (65) is monotonic for all k, as shown in Fig. 6, and the monotonic neutral curve attains its minimal value at $k=0$.

D. Experimental observability of the results

The results of the linear stability analysis given earlier in this section can be expressed in terms of possible experiments with a binary mixture of water-ethanol whose relevant thermophysical properties, such as the Soret diffusion parameter S_T and the gradients of surface tension with respect to both temperature and solute concentration are documented in the literature [19,20] and summarized in Table II.

TABLE II. Material properties for the water-ethanol mixture.

Case I $-c_{wt}=0.2$	Case II $-c_{wt}=0.3$
$c_{mol}=0.1$	$c_{mol}=0.17$
$\sigma_t=1.5\times10^{-4}$ N m^{-1} K^{-1},	$\sigma_t=1.5\times10^{-4}$ N m^{-1} K^{-1}
$\sigma_c=-0.1$ N m^{-1}(mole %)$^{-1}$. Ref. [20]	$\sigma_c=-0.03$ N m^{-1}(mole %)$^{-1}$. Ref. [20]
$S_T=0.003$ K^{-1}, Ref. [19]	$S_T=-0.001$ K^{-1}, Ref. [19]
$\chi=-0.41$	$\chi=0.06$

The mixture water-ethanol is chosen here with the ethanol weight concentration c_{wt} of 0.2 and 0.3 denoted as case I and II, respectively. In these cases, the Soret diffusion coefficient $\alpha=S_T/c_{\mathrm{wt}}$ are of different sign [19]. Based on the molecular weights of ethanol and water 46 and 18, respectively, the mole fraction of ethanol is given by

$$c_{\mathrm{mol}}=\frac{9c_{\mathrm{wt}}}{23(1-c_{\mathrm{wt}})}. \tag{67}$$

The values of σ_t and σ_c are evaluated from the data presented in Ref. [20]. The Lewis number of the mixture is estimated as $L=9.0\times10^{-3}$. The heat transfer rate at the liquid-gas interface used in the computation is $q=10\ \mathrm{W/(m^2\ K)}$. It is stressed that the value of the Biot number B was assumed here to be order one, i.e., not scaled with respect to ε, therefore our results are expected to be valid for all finite values of $B\geqslant0$. The actual value of B is small, $O(10^{-3})$ for the range of the layer thicknesses considered below.

The assumption of small Galileo numbers is valid for thin layers in low gravity. The thresholds of monotonic and oscillatory instabilities are calculated below using Eqs. (34) and (36), respectively, in terms of original, prior to scaling with ε^2, values of the Marangoni number as function of G, L and the rest of parameters.

In case I, for $b_0=1$, $h_0=3.0\times10^{-5}$ m and gravity of $0.01g_0$, where g_0 is the terrestrial gravity acceleration, the value of the Galileo number is $G=2.0\times10^{-2}$ and the instability is monotonic, $M_0=0.024<M_{\mathrm{osc}}=0.11$. The threshold of instability corresponds to the temperature gradient of $a=0.2$ K/cm. In the limit of $b_0=0$ discussed in Ref. [15] the instability would be oscillatory if heating is applied at the gas side with $|M_{\mathrm{osc}}|=0.31<|M_0|=1.05$ corresponding to $a=-3.3$ K/cm, provided that the lateral extent of the system is at least 70 times larger that the film thickness. The limitation for the lateral size of the system comes from the requirement that the value of Ω_0^2 given by Eq. (37) be positive which implies a condition for the critical value for the wave number K.

In case II, with $b_0=1$, $h_0=7.0\times10^{-5}$ m and gravity of $g=10^{-3}g_0$, we find that the instability is monotonic with the threshold $M_0=0.016<M_{\mathrm{osc}}=0.023$ that corresponds to $a=0.03$ K/cm. Furthermore, increasing the film to 9.0×10^{-5} m with the rest of parameters fixed, leads to the change of the instability type from monotonic to oscillatory, $M_{\mathrm{osc}}=0.023<M_0=0.035$ that materializes at $a=0.025$ K/cm. In the limit of $b_0=0$ discussed in Ref. [15] in both of the cases the instability would be oscillatory with $M_{\mathrm{osc}}=0.6<M_0=7.05$ corresponding to $a=1.1$ K/cm provided that the lateral extent of the system is at least 70 times larger that the film thickness.

IV. DERIVATION OF THE LONG-WAVE NONLINEAR EVOLUTION EQUATIONS

A set of three-dimensional governing equations with the corresponding boundary conditions in dimensionless form are given in Eqs. (14)–(16). The perturbation functions (u,v,w,T,C) in the vicinity of the base state (18) satisfy the equations

$$u_x+v_y+w_z=0, \tag{68a}$$

$$u_t+P^{-1}(uu_x+vu_y+wu_z)=-p_x+u_{xx}+u_{yy}+u_{zz}, \tag{68b}$$

$$v_t+P^{-1}(uv_x+vv_y+wv_z)=-p_x+v_{xx}+v_{yy}+v_{zz}, \tag{68c}$$

$$w_t+P^{-1}(uw_x+vw_y+ww_z)=-p_z+w_{xx}+w_{yy}+w_{zz}, \tag{68d}$$

$$PT_t+uT_x+vT_y-w+wT_z=T_{xx}+T_{yy}+T_{zz}, \tag{68e}$$

$$L^{-1}(PC_t+uC_x+vC_y+\chi w+wC_z)=C_{xx}+C_{yy}+C_{zz}+\chi(T_{xx}+T_{yy}+T_{zz}) \tag{68f}$$

and the boundary conditions

$$z=0{:}u=v=w=0,\quad T_z=bT,\quad C_z+\chi T_z=0, \tag{69a}$$

$$z=h(x,y,t){:}-h_xT_x-h_yT_y+T_z+B(T-h+1)\sqrt{1+h_x^2+h_y^2}=0, \tag{69b}$$

$$-h_xC_x-h_yC_y+C_z-\chi B(T-h+1)\sqrt{1+h_x^2+h_y^2}=0, \tag{69c}$$

$$Ph_t+uh_x+vh_y=w, \tag{69d}$$

$$2(w_z-u_x)h_x-(u_y+v_x)h_y-h_yh_x(v_z+w_y)+(u_z+w_x)(1-h_x^2)=M[C_x-T_x+h_x(\chi+1+C_z-T_z)]\sqrt{1+h_x^2+h_y^2}, \tag{69e}$$

$$2(w_z-v_y)h_y-(u_y+v_x)h_x-h_yh_x(u_z+w_x)+(v_z+w_y)(1-h_y^2)=M[C_y-T_y+h_y(\chi+1+C_z-T_z)]\sqrt{1+h_x^2+h_y^2}, \tag{69f}$$

$$[-p+G(h-1)](1+h_x^2+h_y^2)+2[u_x(h_x^2-1)+v_y(h_y^2-1)+(u_y+v_x)h_xh_y-(w_y+v_z)h_y-h_x(u_z+w_x)]=\Sigma\frac{h_{xx}(1+h_y^2)+h_{yy}(1+h_x^2)-2h_xh_yh_{xy}}{(1+h_x^2+h_y^2)^{3/2}}. \tag{69g}$$

The kinematic boundary condition (69d) is rewritten in the conservative form

$$Ph_t=-\frac{\partial}{\partial x}\left[\int_0^h u(x,y,z,t)dz\right]-\frac{\partial}{\partial y}\left[\int_0^h v(x,y,z,t)dz\right]. \tag{70}$$

Integrating Eq. (68f) across the liquid layer, taking into consideration the boundary conditions (69a)–(69d) and introducing the total solute concentration

$$\Gamma = \int_0^h (C + \chi z) dz \tag{71}$$

as a new variable, leads to the second nonlinear evolution equation in the conservative form

$$P\Gamma_t + \frac{\partial}{\partial x}\int_0^h [u(C+\chi z)]dz + \frac{\partial}{\partial y}\int_0^h [v(C+\chi z)]dz - L\frac{\partial}{\partial x}\int_0^h (C_x + \chi T_x)dz - L\frac{\partial}{\partial y}\int_0^h (C_y + \chi T_y)dz = 0. \tag{72}$$

Based on the results of Sec. III, we consider the long-wave Marangoni instability of the system scaling the space and time variables as

$$\xi = \varepsilon x, \quad \eta = \varepsilon y, \quad \tau = \varepsilon^4 t. \tag{73}$$

The problem parameters such as the Lewis, Galileo, Biot, and capillary numbers are scaled as

$$L = \varepsilon^2 l, \quad G = \varepsilon^2 g, \quad B = O(1), \quad b = b_0 + \varepsilon^2 b_2 + \cdots, \quad \Sigma = O(1), \tag{74}$$

where

$$b_2 = -\frac{\tilde{\lambda}\tilde{h}}{3}\left(\frac{\partial^2}{\partial \xi^2} + \frac{\partial^2}{\partial \eta^2}\right). \tag{75}$$

In accordance with the results of the linear theory, the emergence of instability is expected for $M = O(\varepsilon^2)$. We thus define

$$M = \varepsilon^2 m. \tag{76}$$

The independent variables of the problem are expanded into series of ε as

$$u = \varepsilon(u_0 + \varepsilon^2 u_2 + \cdots), \quad v = \varepsilon(v_0 + \varepsilon^2 v_2 + \cdots), \quad w = \varepsilon^2(w_0 + \varepsilon^2 w_2 + \cdots), \tag{77a}$$

$$(T, C, p) = (T_0, C_0, p_0) + \varepsilon^2(T_2, C_2, p_2) + \cdots, \tag{77b}$$

$$h(x,y,t) = 1 + \zeta_0(x,y,t) + \varepsilon^2\zeta_2(x,y,t) = h_0(x,y,t) + \varepsilon^2 h_2(x,y,t) + \cdots. \tag{77c}$$

Equations (76) and (77) are substituted into Eqs. (68)–(70) and (72) and a hierarchy of problems at orders $\varepsilon^0, \varepsilon^2, \ldots$, is obtained and solved.

At leading order with respect to ε, Eqs. (68) and (69) are solved and the solution reads

$$u_0 = v_0 = w_0 = 0, \quad p_0 = 0, \tag{78a}$$

$$T_0 = \frac{B(1 + zb_0)[h_0(\xi,\eta,\tau) - 1]}{B + b_0[1 + Bh_0(\xi,\eta,\tau)]}, \tag{78b}$$

$$C_0 = A(\xi,\eta,\tau) - \frac{Bz\chi b_0[h_0(\xi,\eta,\tau) - 1]}{B + b_0[1 + Bh_0(\xi,\eta,\tau)]}, \tag{78c}$$

where $A(\xi, \eta, \tau)$ is an unknown function.

Solution of Eqs. (68) is carried out up to second order and its results are subsequently substituted into the leading order of Eqs. (70) and (72) to derive the set of long-wave nonlinear evolution equations that govern the spatiotemporal dynamics of a thin binary-liquid film

$$Ph_\tau = \vec{\nabla}_\perp \cdot \vec{\mathbf{Q}}_1, \quad P\Gamma_\tau = \vec{\nabla}_\perp \cdot \vec{\mathbf{Q}}_2, \tag{79}$$

where

$$\vec{\nabla}_\perp = \vec{\mathbf{i}}\frac{\partial}{\partial \xi} + \vec{\mathbf{j}}\frac{\partial}{\partial \eta}, \tag{80}$$

$$\vec{\mathbf{Q}}_1 = \frac{1}{3}gh_0^3\vec{\nabla}_\perp h_0 - \frac{m(2h\beta_1^2\vec{\nabla}_\perp\Gamma - \{2\Gamma\beta_1^2 - \beta_2[B\chi + (2+\chi)b_0]h_0^2\}\vec{\nabla}_\perp h_0)}{4\beta_1^2} - \frac{1}{3}\Sigma h_0^3\vec{\nabla}_\perp\vec{\nabla}_\perp^2 h_0, \tag{81}$$

$$\vec{\mathbf{Q}}_2 = \frac{1}{24h_0\beta_1^3}[m(\chi\beta_2 h^2 + 6\Gamma\beta_1)(2h_0\beta_1^2\vec{\nabla}_\perp\Gamma + \{\beta_2[B\chi + (2+\chi)b_0]h_0^2 - 2\Gamma\beta_1^2\}\vec{\nabla}_\perp h_0)] - \frac{gh_0^2(\chi\beta_2 h_0^2 + 8\Gamma\beta_1)\vec{\nabla}_\perp h_0}{24\beta_1} + \frac{\Sigma h_0^2\beta_2(\chi h_0^2 + 8\Gamma)\vec{\nabla}_\perp\vec{\nabla}_\perp^2 h_0}{24\beta_1} - \frac{1}{2h_0\beta_1^2}(l\{2h_0\vec{\nabla}_\perp\Gamma - [2\Gamma\beta_1^2 - \chi(B - b_0)\beta_2]h_0^2\}) \tag{82}$$

and

$$\beta_1 = B + b_0(1 + Bh_0), \quad \beta_2 = B + b_0(1 + B). \tag{83}$$

It should be noted here that for $b_0 = 0$ which corresponds to the case of low conductivity of the solid substrate, the results presented here reproduce those of Ref. [15].

We now discuss the region of validity of Eqs. (79). To achieve this goal, they are linearized in the vicinity of the base state given by the mean values of both the film depth and solute concentration

$$h(\xi,\eta,\tau) = 1 + H(\xi,\eta,\tau), \quad \Gamma(\xi,\eta,\tau) = \frac{\chi}{2} + c(\xi,\eta,\tau) \tag{84}$$

with $H(\xi, \eta, \tau)$, $c(\xi, \eta, \tau) \ll 1$, resulting in

$$PH_\tau = \vec{\nabla}_\perp \cdot \vec{\mathbf{Q}}_1^{(l)}, \quad Pc_\tau = \vec{\nabla}_\perp \cdot \vec{\mathbf{Q}}_2^{(l)}, \tag{85}$$

where

$$\vec{\mathbf{Q}}_1^{(l)} = -\frac{1}{12}\left\{-4g\vec{\nabla}_\perp H + 3m\left[2\vec{\nabla}_\perp c - \frac{1}{\beta_2}(B\chi - 2)b_0\vec{\nabla}_\perp H\right] + 4\Sigma\vec{\nabla}_\perp\vec{\nabla}_\perp^2 H\right\}, \tag{86}$$

$$\vec{\mathbf{Q}}_2^{(l)} = \frac{1}{24}\left[\frac{1}{\beta_2}(\chi\{5Bg + b_0[5(1+B)g - 12(2+B)l + 4(B\chi - 2)m]\}\vec{\nabla}_\perp H) + 8(3l - \chi m)\vec{\nabla}_\perp c - 5\Sigma\chi\vec{\nabla}_\perp\vec{\nabla}_\perp^2 H\right]. \tag{87}$$

Introducing normal perturbations

$$H(\xi,\eta,\tau) = \Theta e^{i\vec{\mathbf{K}}\cdot\vec{\mathbf{r}}+\omega\tau}, \quad c(\xi,\tau) = \gamma e^{i\vec{\mathbf{K}}\cdot\vec{\mathbf{r}}+\omega\tau}, \tag{88}$$

where $\vec{\mathbf{r}}=(\xi,\eta)$, yields the following set of equations for the amplitudes of the perturbation functions:

$$\frac{1}{12}\left[4(gK^2 + K^4\Sigma + 3P\omega) + \frac{3K^2 m}{\beta_2}(B\chi - 2)b_0\right]\Theta - \frac{1}{2}K^2 m\gamma = 0, \tag{89a}$$

$$\frac{K^2\chi}{24\beta_2}\{5B(g + K^2\Sigma) + [5(1+B)g - 12(2+B)l + 5(1+B)K^2\Sigma + 4m(B\chi - 2)]b_0\}\Theta + \left[K^2 l + P\omega - \frac{1}{3}K^2\chi m\right]\gamma = 0. \tag{89b}$$

Thus, the solvability condition for Eqs. (89) coincides with the dispersion relation given by Eq. (29). The analysis reproduces the results obtained in the previous sections in the framework of the long-wave linear stability theory, Eqs. (33), (36), and (37). Based on Eqs. (32), we conclude that the set of Eqs. (79) is well posed for $m\chi < 48l$ and ill posed for $m\chi > 48l$. Hence, the set of nonlinear evolution equations (79)–(83) shall be used for the domain $m\chi < 48l$. Numerical solution of Eqs. (79)–(83) is outside the scope of this paper and its results will be reported elsewhere. Equations (79)–(83) cannot be used to investigate the domain of $m\chi > 48l$, and therefore a different evolution equation must be derived for that. This task is pursued next.

V. NONLINEAR EVOLUTION OF MONOTONIC INSTABILITY FOR $m\chi > 48l$

We use the scaling based on the results of the linear theory in the domain of $k=O(1)$ for Eqs. (68) and (69)

$$L = \varepsilon^2 l, \quad G = \varepsilon^2 g, \quad M = \varepsilon^2 m, \quad B = O(1), \quad b = O(1),$$

$$\Sigma = O(1), \tag{90a}$$

$$C = \hat{C} + \varepsilon^2\hat{C}_2, \quad (T,u,v,w,p) = \varepsilon^2(\hat{T},\hat{u},\hat{v},\hat{w},\hat{p}), \tag{90b}$$

$$h = 1 + \varepsilon^2\hat{\zeta}, \quad \frac{\partial}{\partial x},\frac{\partial}{\partial y},\frac{\partial}{\partial z} = O(1), \quad \frac{\partial}{\partial t} = O(\varepsilon^2). \tag{90c}$$

At leading order, we obtain a set of equations with boundary conditions

$$\hat{u}_x + \hat{v}_y + \hat{w}_z = 0, \tag{91a}$$

$$-\hat{p}_x + \hat{u}_{xx} + \hat{u}_{yy} + \hat{u}_{zz} = 0, \tag{91b}$$

$$-\hat{p}_y + \hat{v}_{xx} + \hat{v}_{yy} + \hat{v}_{zz} = 0, \tag{91c}$$

$$-\hat{p}_z + \hat{w}_{xx} + \hat{w}_{yy} + \hat{w}_{zz} = 0, \tag{91d}$$

$$\hat{T}_{xx} + \hat{T}_{yy} + \hat{T}_{zz} + w = 0, \tag{91e}$$

$$l^{-1}(P\hat{C}_t + \hat{u}\hat{C}_x + \hat{v}\hat{C}_y + \chi\hat{w} + \hat{w}\hat{C}_z) = \hat{C}_{xx} + \hat{C}_{yy} + \hat{C}_{zz}, \tag{91f}$$

$$z=0{:}\hat{u} = \hat{v} = \hat{w} = 0, \quad \hat{T}_z = b\hat{T}, \quad \hat{C}_z = 0, \tag{92a}$$

$$z=1{:}\hat{T}_z + B(\hat{T} - \zeta) = 0, \tag{92b}$$

$$\hat{C}_z = 0, \quad w = 0, \tag{92c}$$

$$\hat{u}_z + \hat{w}_x = m\hat{C}_x, \tag{92d}$$

$$\hat{v}_z + \hat{w}_y = m\hat{C}_y, \tag{92e}$$

$$-\hat{p} - 2(\hat{u}_x + \hat{v}_y) = \Sigma(\hat{\zeta}_{xx} + \hat{\zeta}_{yy}). \tag{92f}$$

Equation (91f) can be recast into the conservative form by integrating it across the layer and using the boundary conditions (92a) and (92c) for the functions $\hat{w}$ and $\hat{C}$

$$P\frac{\partial}{\partial t}\left[\int_0^1 (\hat{C} + \chi z)dz\right] + \vec{\nabla}\cdot\int_0^1 [\vec{\hat{\mathbf{v}}}(\hat{C} + \chi z) - l\vec{\nabla}\hat{C}]dz = 0. \tag{93}$$

To investigate the weakly nonlinear evolution of the long-wave monotonic instability in the domain $\sqrt{L} \ll k \ll 1$, we employ the scaling

$$k = O(\delta) \ll 1, \quad m = m_0 + \delta^2 m_2 + \cdots, \tag{94a}$$

$$\hat{C} = C_0 + \delta^2 C_2 + \cdots, \quad \hat{T} = \delta^{-2}(T_0 + \delta^2 T_2), \tag{94b}$$

$$(\hat{u},\hat{v}) = \delta(u_1,v_1) + \delta^3(u_3,v_3) + \cdots, \quad \hat{w} = \delta^2 w_2 + \delta^4 w_4 + \cdots, \tag{94c}$$

$$\hat{p} = p_0 + \delta^2 p_2 + \cdots, \quad \hat{\zeta} = \delta^{-2}(\zeta_0 + \delta^2\zeta_2 + \cdots), \tag{94d}$$

$$\frac{\partial}{\partial x} = \delta\frac{\partial}{\partial\xi}, \quad \frac{\partial}{\partial y} = \delta\frac{\partial}{\partial\eta}, \quad \frac{\partial}{\partial t} = \delta^2\frac{\partial}{\partial t_2} + \delta^4\frac{\partial}{\partial t_4}. \tag{94e}$$

It is important to emphasize here that in spite of apparently large values for the disturbances T and ζ in Eqs. (94) due to the factor δ^{-2}, it follows from scalings (90) and (94) that in the relevant domain of $\sqrt{L}=O(\varepsilon) \ll k=O(\delta) \ll 1$, both T and ζ are in fact scaled with $(\varepsilon/\delta)^2 \ll 1$. Therefore they are asymptotically small, as expected.

At zero order Eq. (93) becomes

$$P\frac{\partial}{\partial t_2}\left[\int_0^1 (C_0+\chi z)dz\right]+\frac{\partial}{\partial \xi}\int_0^1 [u_1(C_0+\chi z)]dz + \frac{\partial}{\partial \eta}\int_0^1 [v_1(C_0+\chi z)]dz - l\frac{\partial}{\partial \xi}\int_0^1 C_{0,\xi}dz - l\frac{\partial}{\partial \eta}\int_0^1 C_{0,\eta}dz = 0, \tag{95}$$

where

$$u_1=\frac{1}{6}z(-2+3z)p_{0,\xi}(\xi,\eta,t_2,t_4),$$

$$v_1=\frac{1}{6}z(-2+3z)p_{0,\eta}(\xi,\eta,t_2,t_4), \tag{96a}$$

$$p_0(\xi,\eta,t_2,t_4)=-\Sigma(\zeta_{0,\xi\xi}+\zeta_{0,\eta\eta}),$$

$$C_0(\xi,\eta,t_2,t_4)=\frac{2p_0(\xi,\eta,t_2,t_4)}{3m_0}. \tag{96b}$$

Hence, after simplifications, Eq. (95) takes the following form:

$$\frac{\partial \zeta_0}{\partial t_2}=\frac{1}{48P}(48l-\chi m_0)\vec{\nabla}^2\zeta_0. \tag{97}$$

Thus, at the instability threshold $m_0=\frac{48l}{\chi}$, the growth rate of the interfacial deformation in time t_2 is zero, i.e., $\frac{\partial \zeta_0}{\partial t_2}=0$.

At the next order of approximation, Eq. (93) yields

$$P\frac{\partial}{\partial t_2}\left[\int_0^1 C_2 dz\right]+P\frac{\partial}{\partial t_4}\left[\int_0^1 (C_0+\chi z)dz\right]+\frac{\partial}{\partial \xi}\int_0^1 [u_1C_2 + u_3(C_0+\chi z)]dz+\frac{\partial}{\partial \eta}\int_0^1 [v_1C_2+v_3(C_0+\chi z)]dz - l\frac{\partial}{\partial \xi}\int_0^1 C_{2,\xi}dz - l\frac{\partial}{\partial \eta}\int_0^1 C_{2,\eta}dz = 0, \tag{98}$$

where

$$C_2(z,\xi,\eta,t_2,t_4)=\Upsilon(\xi,\eta,t_2,t_4)+\frac{\chi}{l^2}(\vec{\nabla}p_0)^2\left\{\frac{z^4}{1728}-\frac{z^3}{1296}\right\}+\frac{\chi}{l}\nabla^2 p_0\left\{\frac{z^4}{72}-\frac{z^2}{144}-\frac{z^5}{120}\right\}, \tag{99a}$$

$$u_3=z\left\{\frac{48l}{\chi}\Upsilon_\xi+\frac{\chi m_2}{72l}p_{0,\xi}-\Pi_{2,\xi}+\frac{1}{10}\nabla^2 p_{0,\xi}-\frac{1}{54l}(p_{0,\eta}p_{0,\xi\eta}+p_{0,\xi}p_{0,\xi\xi})\right\}+\frac{z^2}{12}\{6\Pi_{2,\xi}-\nabla^2 p_{0,\xi}\}+\nabla^2 p_{0,\xi}\left\{\frac{z^3}{9}-\frac{z^4}{12}\right\}, \tag{99b}$$

$$v_3=z\left\{\frac{48l}{\chi}\Upsilon_\eta+\frac{\chi m_2}{72l}p_{0,\eta}-\Pi_{2,\eta}+\frac{1}{10}\nabla^2 p_{0,\eta}-\frac{1}{54l}(p_{0,\xi}p_{0,\xi\eta}+p_{0,\eta}p_{0,\eta\eta})\right\}+\frac{z^2}{12}\{6\Pi_{2,\eta}-\nabla^2 p_{0,\eta}\}+\nabla^2 p_{0,\eta}\left\{\frac{z^3}{9}-\frac{z^4}{12}\right\}, \tag{99c}$$

$$\Pi_2(\xi,\eta,t_2,t_4)=-\Sigma\nabla^2\zeta_2(\xi,\eta,t_2,t_4), \tag{99d}$$

$$\Upsilon(\xi,\eta,t_2,t_4)=\frac{\chi}{72l}\Pi_2(\xi,\eta,t_2,t_4)+\Phi(\xi,\eta,t_2,t_4), \tag{99e}$$

$$\Phi(\xi,\eta,t_2,t_4)=-\frac{\chi^2 m_2}{3456l^2}p_0-\frac{\chi}{720l}\nabla^2 p_0+\frac{\chi}{5184l^2}(\vec{\nabla}p_0)^2. \tag{99f}$$

Using Eqs. (99) the evolution equation (98) is rewritten in the form

$$P\frac{\partial C_0}{\partial t_4}=-\frac{\chi m_2}{48}\nabla^2 C_0-\frac{l}{15}\nabla^4 C_0+\frac{48l}{35\chi^2}\vec{\nabla}[\vec{\nabla}C_0\cdot(\vec{\nabla}C_0)^2] + \frac{l}{10\chi}\vec{\nabla}[\vec{\nabla}C_0\cdot\nabla^2 C_0]+\frac{3l}{5\chi}\nabla^2[(\vec{\nabla}C_0)^2]. \tag{100}$$

In the two-dimensional case all these expressions are significantly simplified. We finally obtain the evolution equation describing the long-wave nonlinear evolution of the monotonic instability in the two-dimensional case

$$P\frac{\partial \Psi}{\partial t_4}+\frac{\partial^2}{\partial \xi^2}\left\{\frac{\chi m_2}{48}\Psi-\frac{48l}{35\chi^2}\Psi^3-\frac{13l}{10\chi}\Psi\Psi_\xi+\frac{l}{15}\Psi_{\xi\xi}\right\}=0, \tag{101}$$

where

$$\Psi=\frac{\partial C_0}{\partial \xi},\quad C_0=-\frac{2\Sigma}{3m_0}\zeta_{0,\xi\xi},\quad m_0=\frac{48l}{\chi}. \tag{102}$$

Equation (101) is similar to the equation derived and studied in the context of the Bénard-Marangoni convection in pure liquids [18].

VI. SUMMARY

Linear and nonlinear stability analysis of the long-wave Marangoni instability of a system that consists of a layer of an incompressible binary liquid with a deformable free surface laying on a solid layer of a finite thickness subjected to differential heating across it is considered in the presence of the Soret effect in the case of a finite Biot number at the liquid-gas interface. The case of a physically relevant limit of a small Lewis number under microgravity conditions is considered here. As shown in our previous paper [15], in this limit both long-wave monotonic and oscillatory modes of instability emerge in the case of low conductivity of the solid substrate. In the present work we consider the case of finite conductivity of the solid substrate and as such, it allows one to bridge between various thermal boundary conditions at the

solid-liquid boundary considered in the literature [9,12–14] for layers of binary liquid.

The long-wave Marangoni instability is investigated in the framework of linear stability theory in the limit of asymptotically small Lewis and Galileo numbers $L,G=O(\varepsilon^2)$ in the domain of wave numbers $k=O(\varepsilon)$. Both long-wave monotonic and oscillatory modes of instability are found in the case of a finite Biot number at the gas-liquid interface and a finite conductivity of the solid substrate. Our analysis reveals a competition between different modes of instability in various parameter domains of Biot and Soret numbers.

Linear stability analysis in the domain of finite wave numbers $k=O(1)$ in the case of asymptotically small Lewis and Galileo numbers reveals that there are no additional minima of the monotonic neutral curve in the domain of $k=O(1)$.

Study of the asymptotic behaviors of the long-wave monotonic neutral curve obtained in the region $k=O(\varepsilon)$ in the limit of large wave numbers and also of the monotonic neutral curve obtained in the case of finite wave numbers $k=O(1)$ in the limit when $k\to 0$, we reveal a long-wave intermediate asymptotic limit $k=O(L^{1/4})=O(\sqrt{\varepsilon})$, where depending on the parameter values the minimum of the full monotonic neutral curve can be present.

A set of long-wave nonlinear evolution equations that governs the spatiotemporal dynamics of a thin binary-liquid film is derived in the domain of $k=O(\varepsilon)$. Our analysis shows that the set of equations is well-posed when the Marangoni number is below the monotonic instability threshold, i.e., $M<48L/\chi$.

A weakly nonlinear evolution equation describing the dynamics of the long-wave monotonic instability is derived in the domain of wave numbers $\sqrt{L}\ll k\ll 1$. The form of the obtained nonlinear evolution equation is very similar to that obtained for the surface-tension driven convection in a horizontal liquid layer confined between poorly conducting boundaries [18].

ACKNOWLEDGMENTS

The research was partially supported by the Israel Science Foundation founded by the Israel Academy of Sciences through Grant No. 31/03-15.3. A.O. acknowledges a partial support by the Technion President Research Fund and the Fund for Promotion of Research at the Technion. A.A.N. acknowledges partial support from the Israel Ministry of Science through Grant No. 3-3570.

[1] S. Ostrach, J. Fluids Eng. **105**, 5 (1983).
[2] J. L. Castillo and M. G. Velarde, Phys. Lett. **66A**, 489 (1978).
[3] M. Takashima, J. Phys. Soc. Jpn. **47**, 1321 (1979).
[4] M. Takashima, J. Phys. Soc. Jpn. **49**, 802 (1980).
[5] J. L. Castillo and M. G. Velarde, J. Non-Equil. Thermodyn. **5**, 111 (1980).
[6] C. F. Chen and C. C. Chen, Phys. Fluids **6**, 1482 (1994).
[7] J. R. L. Skarda, D. Jacqmin, and F. E. McCaughan, J. Fluid Mech. **366**, 109 (1998).
[8] S. Slavchev, G. Simeonov, S. Van Vaerenbergh, and J. C. Legros, Int. J. Heat Mass Transfer **42**, 3007 (1999).
[9] A. Oron and A. A. Nepomnyashchy, Phys. Rev. E **69**, 016313 (2004).
[10] S. R. de Groot and P. Mazur, *Non-Equilibrium Thermodynamics* (North-Holland, Amsterdam, 1969).
[11] M.-I. Char and K.-T. Chiang, Int. J. Heat Mass Transfer **39**, 407 (1996).
[12] J. K. Bhattacharjee, Phys. Rev. E **50**, 1198 (1994).
[13] S. W. Joo, J. Fluid Mech. **293**, 127 (1995).
[14] A. Podolny, A. Oron, and A. A. Nepomnyashchy, Phys. Fluids **17**, 104104 (2005).
[15] A. Podolny, A. Oron, and A. A. Nepomnyashchy, Phys. Fluids **18**, 054104 (2006).
[16] B. J. A. Zielinska and H. R. Brand, Phys. Rev. A **35**, 4349 (1987).
[17] J. Lenglet, A. Bourdon, J. C. Bacri, and G. Demouchy, Phys. Rev. E **65**, 031408 (2002).
[18] L. Shtilman and G. I. Sivashinsky, Physica D **52**, 477 (1991).
[19] P. Kolodner, H. Williams, and C. Moe, J. Chem. Phys. **88**, 6512 (1988).
[20] M. Aratono, T. Toyomasu, M. Villeneuve, Y. Uchizono, T. Takiue, K. Motomura, and N. Ikeda, J. Colloid Interface Sci. **191**, 146 (1997).